Published in final edited form as:
Brain Res. 2012 February 27; 1440: 1–8. doi:10.1016/j.brainres.2011.12.034.

Developmentally Altered Inhibition in Ts65Dn, a mouse model of Down syndrome

Ananya Mitra[1], **Martina Blank**[2], and **Daniel V. Madison**[1]

[1]Department of Molecular and Cellular Physiology, Stanford University School of Medicine, Stanford, California, USA 94305

[2]Department of Psychiatry and Behavioral Sciences, Stanford University School of Medicine, Stanford, California, USA 94305

Abstract

We studied the development of GABA-mediated synaptic inhibition in the CA1 region of the hippocampus in Ts65Dn mice, a model system for Down syndrome (DS). While there was no significant difference in the amplitude of stimulus-evoked monosynaptic inhibitory postsynaptic potentials (IPSPs) between acute hippocampal slices from Ts65Dn mice and diploid (2N) wild-type littermates at the end of the first and third postnatal week, the Ts65Dn animals showed significantly larger inhibitory responses when compared to age-matched controls at the end of the second postnatal week. This transient change in evoked inhibition was strikingly layer specific, observed only when stimulating in the *strata radiatum* and *pyramidale* but not in the *stratum oriens*. In addition, the frequency (but not amplitude) of spontaneous action-potential independent miniature inhibitory postsynaptic currents (mIPSCs) was significantly increased in the Ts65Dn mice during the second postnatal week. Additional measurements of paired pulse ratios showed no significant difference between the genotypes. We conclude that the excess inhibition at the end of the second postnatal week in Ts65Dn mice is not due to increases in release probability or post-synaptic quantal size. Overall these experiments indicate that there is a specific disruption of the normal developmental progression of inhibitory synaptic transmission in Ts65Dn mice at a critical time point in the development of neuronal circuitry. This raises the possibility that a transient early disruption of inhibitory function may have lasting impact on other network properties and could contribute to later neural circuit dysfunction in DS.

Keywords

postnatal development; CA1; inhibitory synaptic transmission; Down syndrome; Hippocampus; GABA; development

Corresponding Author: Dr. Daniel V. Madison, Department of Molecular and Cellular Physiology, Stanford University School of Medicine, Stanford, CA USA 94305-5345, Phone +1-(650) 725-7545, Fax +1(650) 618-2779, madison@stanford.edu.

1. INTRODUCTION

Down syndrome (DS) is caused by triplication of human chromosome 21 and occurs in approximately 1 out of every 715 live births in the United States (Canfield et al., 2006; Parker et al., 2010). The complete DS phenotype is complex, affects multiple organ systems, and is variable in severity. A common feature among people with DS is cognitive dysfunction leading to intellectual disabilities both in children and adults (Pennington et al., 2003). Early neuro-developmental changes are likely to contribute to intellectual disability in DS. The volume of DS brain is reduced as early as 4–5 months *in utero* (Guihard-Costa et al., 2006; Winter et al., 2000). A selective decrease of the hippocampus and temporal lobe has been revealed through MRI studies in children and young individuals with DS (Jernigan and Bellugi, 1990; Kates et al., 2002; Pinter et al., 2001a; Pinter et al., 2001b). The number of neurons is reduced in the hippocampus, parahippocampal gyrus, and neocortex of DS fetuses (Guidi et al., 2008; Larsen et al., 2008) and in the cortex of DS children (Wisniewski, 1990). A combination of decreased neurogenesis and increased apoptosis contribute towards the hypocellularity in the DS brain (Contestabile et al., 2007; Guidi et al., 2008). At the cellular level, changes in length and branching of dendrites, and number and shape of dendritic spines appear early in development (Becker et al., 1991; Becker et al., 1986; Marin-Padilla, 1976; Takashima et al., 1981; Takashima et al., 1989). Biochemically, alterations of several neurotransmitter systems have been reported in DS fetuses (Whittle et al., 2007).

To address the mechanisms underlying cognitive dysfunction in DS, several mouse models of human trisomy 21 have been created through genetic manipulation of mouse chromosome 16 (MMU16), which contains many of the evolutionarily conserved genes of human chromosome 21 (HSA21) (Davisson et al., 1993). The Ts65Dn mouse carries an extra chromosome fragment composed of the distal part of MMU16 attached to the centromeric portion of MMU17. This fragment contains about half of the HSA21 genes (136 orthologs) (Antonarakis et al., 2004; Reeves, 2006). The Ts65Dn mouse is the best-characterized of DS models and exhibits several of the phenotypes seen in humans with DS, including memory deficits involving the hippocampus. Behaviorally, Ts65Dn mice show cognitive impairment and display difficulties performing tasks requiring long-term, but not short-term memory (Fernandez and Garner, 2008; Fernandez et al., 2007) indicating that hippocampus-dependent learning and memory is impaired. Possible anatomical correlates of impaired hippocampal function may include changes in the number of principal neurons in CA3 and the dentate gyrus in adult Ts65Dn mice (Insausti et al., 1998; Lorenzi and Reeves, 2006) as well as changes in the number of excitatory synapses in CA1, CA3, and dentate gyrus in aged Ts65Dn mice (Kurt et al., 2004).

Previous studies from our laboratory showed an increased inter-connectivity of CA3 pyramidal neurons but a reduction in overall spontaneous excitatory and inhibitory inputs to these neurons in organotypic hippocampal slices from neonatal Ts65Dn (Hanson et al., 2007). Defects of synaptic plasticity have also been reported in CA1 and dentate gyrus of the Ts65Dn hippocampus. Reduced long-term potentiation (LTP) and increased long-term depression (LTD) have been observed in CA1 of 2 month old Ts65Dn mice (Siarey et al., 1999; Siarey et al., 1997). LTP induction is also impaired in the dentate gyrus of adult

Ts65Dn mice (Kleschevnikov et al., 2004), but can be restored by blocking $GABA_A$ receptors acutely or chronically (Fernandez et al., 2007; Kleschevnikov et al., 2004). In addition, chronic administration of $GABA_A$ antagonists has been shown to improve hippocampal-dependent learning and memory in Ts65Dn mice (Fernandez et al., 2007). These studies strongly suggest that excess inhibition may preclude LTP induction and reduce cognitive performance in adult Ts65Dn mice.

Currently, it is unclear *when* during development excess inhibition arises, and the synaptic properties that may result in this inhibitory dysfunction are not well characterized. Here, we study $GABA_A$ receptor mediated inhibition in the CA1 area of the Ts65Dn hippocampus, looking at layer specific changes in synaptic inhibition at different developmental times, and some of the synaptic properties that may influence these changes.

2. RESULTS

2.1 Layer specific alteration in inhibitory synaptic transmission in CA1 region of Ts65Dn mice

We examined inhibitory synaptic transmission in Ts65Dn mice and 2N (diploid, wild-type) littermate controls by recording stimulus-evoked monosynaptic inhibitory postsynaptic potentials (IPSPs) in CA1 pyramidal cells from acute hippocampal slices obtained from two-week postnatal (P14–16) mice. The resting membrane potential was similar in 2N (−72.9 ± 0.5 mV) and Ts65Dn (−74.5 ± 0.7 mV) CA1 neurons after correcting for electrode liquid junction potential (apparent membrane potentials were −60.1 mV and −61.7 mV for 2N and Ts65Dn, respectively). Since the amplitude of IPSPs strongly depends on membrane potential, for the evoked IPSP experiments, we injected a bias current to move cells to an apparent membrane potential of −60 mV, if necessary (which was −73 mV after liquid junction potential correction), before delivering the stimulus. Thus, all IPSPs in 2N and Ts65Dn slices were measured at the same membrane potential. By stimulating in three different layers of CA1 region (*strata oriens*, *pyramidale*, *and radiatum*, Fig. 1a) while recording from an excitatory CA1 pyramidal cell, we were able to excite subsets of interneurons residing in the different hippocampal layers and compare the relative inhibitory responses from interneurons. In the presence of AMPA and NMDA receptor antagonists (10 μM NBQX and 50 μM AP-5, respectively), we recorded monosynaptic IPSPs in whole-cell recordings from CA1 pyramidal neurons evoked by brief (100 μs) electrical stimulation delivered through a concentric bipolar metal (platinum-iridium) stimulating electrode placed in the appropriate layer approximately 250 μm (unless otherwise noted) from the recording electrode. The IPSPs were due to $GABA_A$ mediated current since they could be blocked by 100 μM picrotoxin, a noncompetitive $GABA_A$ channel blocker (data not shown). Fig. 1b depicts exemplar IPSP traces in response to increasing stimulation intensities ranging from 10–300 μA. Evoked inhibitory transmission in Ts65Dn mice was indistinguishable from that in 2N littermates when we stimulated interneurons in the *s. oriens* (Fig. 1c, f). However, when we stimulated in the *s. radiatum* or *pyramidale*, we found slices from Ts65Dn mice to have significantly greater inhibition than slices obtained from 2N animals. Stimulation in the *s. radiatum* of Ts65Dn tissue yielded monosynaptic IPSPs that were on average nearly double those in 2N tissue (2N: −5.42±0.39mV; Ts65Dn: −9.73±1.3mV) at 300 μA stimulus

intensity (n=8, 2N; n=7, Ts65Dn, where 'n' refers to the total number of animals; $P < 0.005$, ANOVA; Fig. 1 d,f). Stimulation in the *s. pyramidale* yielded less but still significant difference between the two genotypes (2N: −6.55±0.58 mV, n=8; Ts65Dn: −8.75±0.45 mV, n=7; $P<0.05$, ANOVA; Fig. 1e,f).

2.2 Developmental time course of basal inhibitory synaptic transmission in CA1 region of Ts65Dn mice

We next set out to determine whether a similar layer specific difference occurs between Ts65Dn and 2N mice observed at P14–16, also occurred at other developmental time-points. We measured evoked monosynaptic IPSPs in slices from animals after the first (P8–10) and third (P19–21) postnatal week. We found no significant difference between the two genotypes in any hippocampal layer during the first postnatal week (2N, n=6; Ts65Dn, n=5 for all the layers). Surprisingly, we also did not find any difference between the two genotypes for the different layers during the third postnatal week (2N, n=7; Ts65Dn, n=7 for all the layers). Thus, significant difference in basal inhibition between the genotypes was observed only at P14–16 and was unique to interneuron stimulation in *s. radiatum* and *s. pyramidale* (Fig. 2).

2.3 Altered inhibitory transmission in Ts65Dn is not due to changes in release probability

The age- and layer-specific increase in the amplitude of monosynaptic-evoked IPSPs in Ts65Dn mice could arise from a number of factors, including a relative increase in neurotransmitter release probability, an increase number or conductance of postsynaptic $GABA_A$ receptors, and/or an increase in the number of inhibitory synapses in Ts65Dn during the second postnatal week. To test for changes in relative release probability, we measured the paired-pulse ratio (PPR) of the evoked inhibitory postsynaptic current (IPSC) in CA1 pyramidal cells voltage clamped at −74 mV (after correcting for liquid junction potential) in response to a pair of stimuli. The PPR is the relative strength of a second IPSC evoked shortly after a prior IPSC. Changes in PPR are often indicative of alterations in presynaptic function caused by a number of factors including presynaptic calcium handling and the number of synaptic vesicles available in a readily-releasable pool (Zucker and Regehr, 2002). In particular, PPR is sensitive to changes in transmitter release probability, with lower ratios being associated with elevated release probability and higher ratios with lower levels of release probability (Zucker and Regehr, 2002). Pairs of stimuli with an inter-stimulus interval ranging from 10 to 200 ms were administered in the *s. radiatum* layer, while recording the IPSCs in CA1 pyramidal neurons from acute slices obtained from P14–16 animals. We did not see any significant change in the PPR between the genotypes over the entire range of inter-stimulus intervals (ISI) tested (2N, n=5; Ts65Dn, n=4; $P > 0.6$, ANOVA; Fig. 3), suggesting that neurotransmitter release probability was similar in Ts65Dn and 2N tissues at P14-P16.

2.4 Frequency of spontaneous AP-independent inhibitory input to CA1 pyramidal neurons is increased in Ts65Dn animals

Given that we observed an excess of evoked inhibition in P14–16 Ts65Dn animals but no change in PPR, we then proceeded to compare spontaneous inhibitory transmission in acute

slices prepared from 2N and Ts65Dn animals in the P14–16 age group to give us insights into other synaptic changes (e.g. an increase post-synaptic quantal size and/or an in the number of functional synapses) that maybe causing this excess inhibition. We recorded spontaneous miniature IPSCs (mIPSCs) from CA1 pyramidal neurons of 2N and Ts65Dn slices using whole-cell voltage-clamp recordings from slices perfused with ACSF containing NBQX (10 μM) and D-APV (50 μM), to block glutamate-dependent synaptic currents, and TTX (1 μM) to block action potential dependent events. Under these conditions, all remaining spontaneous synaptic currents were blocked by picrotoxin (100 μM; data not shown), confirming that the recorded events were $GABA_A$-mediated mIPSCs. The frequency of mIPSCs was significantly higher in Ts65Dn slices compared with slices from 2N littermates (average frequency, 2N, 2.07 ± 0.21 Hz; n= 7; Ts65Dn, 3.24 ± 0.36 Hz; n = 5; $P < 0.05$, unpaired *t*-test; Fig. 4a). Given that we saw no change in PPR in the two genotypes, the most likely explanation for the increase in mIPSC frequency is an increase in the number of functional synapses in the Ts65Dn animals as compared to 2N at P14-P16. The increase in mIPSC frequency was not accompanied by an alteration in the amplitude of these events, as seen in cumulative probability histograms (Fig. 4b), suggesting that unitary post-synaptic size remained unchanged in the two genotypes.

3. DISCUSSION

In this study we examined the postnatal development of GABAergic inhibition in the hippocampus of Ts65Dn mice at three different developmental time points: P8–10, P14–16, and P19–21. We found a relatively heightened inhibition at age P14–16 but not at ages P8–10 or P19–21. Furthermore, we find that the pronounced excess of inhibition at P14–16 was due to a subclass of interneurons and/or their axons localized to the *s. radiatum* and to a lesser extent in the *s. pyramidale* (Fig. 1).

3.1 Significance of age specificity

Synaptogenesis occurs in the hippocampus and cortex starting at P8 with inhibitory synaptogenesis preceding excitatory synapses formation (Ben-Ari, 2002; Tyzio et al., 1999). This exuberant period of synaptogenesis is followed by pruning to attain the synapse numbers found in adults. Pruning of both excitatory and inhibitory synapses have been shown to occur in the cortex, though inhibitory synapses are less affected by the pruning process (De Felipe et al., 1997). Our data suggest that perhaps in the Ts65Dn, the rate of pruning of inhibitory synapses is delayed resulting in the transient excess of inhibition at P14–16 that we observed.

Alternatively, development of pyramidal cells in CA1 could be accelerated leading to a larger proportion of mature neurons with more developed apical dendrites. Since inhibitory synapses are first formed on the apical dendrites of pyramidal cells followed by synapse formation onto the soma, this scenario would lead to a transient increase in inhibition (Ben-Ari, 2002). One example of such accelerated development of pyramidal neurons in DS stems from studies in human infants and children with DS. While in 4–6 month old infants increased branching and total length of apical and basal dendrites has been reported, DS children older than 2 years of age show dendritic complexity below normal levels (Becker et

al., 1986). Furthermore, in brains of neonate Ts65Dn mice the levels of the dendritic marker, microtubule-associated protein 2 (MAP2), is increased compared to 2N littermate controls (Pollonini et al., 2008). By 4 months of age, MAP2 levels in Ts65Dn hippocampus are comparable to 2N, and by 9 months levels are relatively decreased in Ts65Dn (Granholm et al., 2003). Together these results support our hypothesis of accelerated dendritic maturation of Ts65Dn neurons early in development.

3.2 Significance of Layer specificity

Interneurons in *s. radiatum* tend to receive inputs from different feedback and feed-forward sources and send their outputs to different hippocampal layers than do *s. oriens* or *s. pyramidale* interneurons (Kullmann, 2011; Nurse and Lacaille, 1997; Parra et al., 1998). The significance of our finding lies in the potential differential regulation of the processes that are shaped by the dendritic inhibition in *s. radiatum*. Interestingly, the synaptic inhibition in the *s. pyramidale* seems to be less affected in the Ts65Dn mice compared with *s. radiatum*. This may reflect differences in the interneurons in these two layers. Alternatively, it can also be argued that the small amount of excess inhibition that we see at P14–16 when we stimulate in the *s. pyramidale* is due to our inability to strictly localize our stimulation to only *s. pyramidale*, given that this layer is very narrow and directly adjacent to *s. radiatum*.

One experimental issue we faced was the physical size of the tissue at different developmental stages. Because of the small size of the slices from animals at age P8–10, we could not position the stimulating electrode any farther than about 150 μm away from the post-synaptic cell. Attempting to position the electrode at a greater distance did not result in a monosynaptic IPSP suggesting that the spread of inhibitory axonal arbors is more modest at this younger age. For animals P14–16 and P19–21 groups, we positioned the stimulating electrode ~ 250 μm away to get the maximal monosynaptic IPSP. Because of these differences in electrode placement, we did not feel confident in comparing the absolute amplitude of IPSPs between different age groups. However, since the electrode distance was kept constant for both 2N and Ts65Dn within each developmental age group, a ratio of the average IPSC from Ts65Dn and 2N (maximal inhibitory synaptic strength in Ts65Dn normalized to the average maximal synaptic strength in 2N animals for each layer and developmental time point) was a more accurate reflection of the changes in inhibitory tone during development.

We measured monosynaptic inhibition by blocking excitatory glutamatergic transmission. Thus the increased inhibition at P14–16 is not due to greater excitatory drive onto the interneurons rather is a result of either an increase in the intrinsic excitability of interneurons or an enhancement of inhibitory synaptic properties (e.g., P_r, postsynaptic quantal amplitude and/or number of synapses) on CA1 pyramidal neurons. We found a significant increase in mIPSC frequency in slices from Ts65Dn mice but no change in mIPSC amplitude suggesting either a presynaptic abnormality or a change in the number of functional inhibitory synapses. Studies aimed at presynaptic measurements such as paired pulse ratio indicated no change in relative release probability. Thus the lack of change paired pulse ratio as well as mIPSC amplitude most strongly points to a change in the number of functional inhibitory synapses as opposed to a strictly pre- or post-synaptic effect.

It is of interest to compare our results with those of Chakrabarti et al., 2010. In contrast to our finding that the frequency of mIPSCs is increased at postnatal days 14–16, they find no change in mIPSC frequency in tissue from 2–3 week old animals. However, they reported an increase in the frequency of action potential-dependent spontaneous IPSCs (sIPSCs), which actually includes both sIPSCs and mIPSCs. It must be noted that this postnatal period between 2 and 3 weeks spans our two time points of P14–16, where we see an increase in mIPSC frequency as well as an increase in evoked IPSP, and P19–21 where we see no change in evoked IPSP. Thus, it is not possible to determine whether our two sets of results disagree or not. Chakrabarti et al. suggest that this increase in sIPSCs is due to an increased number of parvalbumin- and somatostatin-positive interneurons in the CA1 region of the Ts65Dn hippocampus at P15. While our data does not rule in or out any change in the number of interneurons, the clear increase in the frequency of mIPSCs that we observed strongly suggests that there are either more inhibitory synapses terminating on a given pyramidal neuron, or that the basal release probability of these inhibitory terminals is elevated compared with 2N controls. Since we see no change in the paired pulse relationship of evoked inhibition between 2N and Ts65Dn tissue, our results suggest that release probability is not affected. Thus, there are more functional inhibitory synapses at P14–16, resulting in the increased evoked inhibition as well as the increase mIPSC frequency that we observe.

This increase in functional synapses could possibly arise from an increase in the number of interneurons, such as that reported by Chakrabarti et al., although our data do not differentiate between the possibility that an increase in the number of inhibitory synapses arises from an increase in the number of interneurons, while keeping the number of synapses per interneuron constant, or an increase in the number of synapses per interneuron with the size of the interneuron population remaining fixed. In this light, it is interesting to note that Chakrabarti et al. report that the increase in the number of interneurons persists to at least P30, well beyond our time-point of P19–21 where we see no change in evoked IPSP. However, it must be noted that they report a number on *hippocampal* interneurons only at P15 (where we see an increased mIPSC frequency). Their measurements of cell number at P8 and P30 were made only in the neocortex and not in hippocampus. Nonetheless, if we suppose that their neocortical data suggest that a similar developmental persistence of an increased number of interneurons also occurs in the hippocampus, then we would hypothesize that despite any change in the overall number of interneurons in the hippocampus, that the number of inhibitory synapses made onto an individual pyramidal neuron is tightly controlled and returns to a basal value shortly after increasing at P14–16.

Overall our findings indicate that there is a specific disruption of the normal developmental progression of inhibitory synaptic transmission in Ts65Dn mice at a critical time point in the development of neuronal circuitry. This raises the possibility that a transient early disruption of inhibitory function may have lasting impact on other network properties and could contribute to later neural circuit dysfunction in DS.

4. EXPERIMENTAL PROCEDURES

4.1 Mouse Breeding and Genotype

Segmental trisomy 16 (Ts65Dn) mice were obtained by mating female carriers of the 17^{16} chromosome (B6EiC3H-a/ATs65Dn) with (C57BL/6JEi×C3H/HeSnJ)F_1 (JAX #JR1875) hybrid males (Davisson et al., 1993). The Ts65Dn and diploid (2N) wild-type littermates were distinguished using quantitative real-time PCR analysis of DNA isolated from tail samples using published protocols (Hanson et al., 2007; Liu et al., 2003).

4.2 Preparation of Acute Hippocampal Slices

Hippocampal slices were prepared from mice P8–10, P14–16, and P19–21 age groups. Hippocampi were dissected from the brain and cut into 300 μm coronal sections using a vibrating sectioning system (Vibratome 3000). Slices were cut in ice-cold modified oxygenated artificial cerebrospinal fluid (ACSF) containing (mM): 210mm sucrose, 2.5 KCl, 1.3 MgSO4, 2.5 CaCl2, 1Na2HPO4, 26.2 NaHCO3 and 11 glucose followed by 30 min. recovery period in ACSF (identical to cutting solution except sucrose is replaced by 119 mM NaCl) at 32°C, prior to storage at room temperature.

4.3 Electrophysiology

During recording, slices were superfused with ACSF at room temperature, containing (mM): 119 NaCl, 2.5 KCl, 1.3 MgSO4, 2.5 CaCl2, 1Na2HPO4, 26.2 NaHCO3, 11 glucose, and 10 μM NBQX and 50 μM D-AP5, perfused at a rate of ~2 ml/ min. Pyramidal cells in area CA1 were visualized by infrared differential interference contrast (DIC) microscopy. Recording electrodes were made of borosilicate glass capillaries (1B150F; World Precision Instruments, Sarasota, FL) and filled with internal electrode solution consisting of (mM): 120 potassium gluconate, 40Hepes, 5 MgCl2, 0.3 NaGTP, 2 NaATP, pH adjusted to 7.2 with KOH for measuring evoked IPSPs in current clamp configuration and 135 CsCl, 2 MgCl2, 2.5 EGTA, 10 HEPES, 2 MgATP, 0.2 Na2-GTP, and 2 lidocaine *N*-ethyl bromide, osmolarity 290, pH 7.3, for measuring miniature and evoked IPSCs in voltage-clamp mode. For evoked IPSCs and PPR measurements, external calcium was reduced from 2.5 to 0.8 mM. To obtain PPR, we measured the amplitude of the first evoked IPSC as the difference between the peak response and the baseline for the recording. The strength of the afferent stimuli was adjusted such that the peak response of the first IPSC was similar in all experiments. The amplitude of the second evoked IPSC was calculated by measuring the peak response after subtracting the average waveform of first IPSC. Five responses were averaged for each paired stimuli. Spontaneous miniature IPSCs were recorded in normal ACSF containing 10 μM NBQX, 50 μM D-AP5, and 1 μM TTX. All experiments were performed at room temperature (22–24°C). The junction potential was 12.4 mV for the current-clamp recordings and 4.1 mV for the voltage clamp recordings. All experiments have been corrected for the junction potential. All electrophysiology data acquisition was done with pClamp10 software suite.

4.4 Data Analysis and statistics

The experimenter was **blind to the genotypes** of the animals during preparation of tissue, data acquisition, and analysis. Current amplitudes were measured at peak deflection relative to baseline using *Clampfit10* (Molecular Devices). Spontaneous miniature IPSCs were detected in the Clampfit program (Axon Instruments) using a template method with a detection threshold of −5 pA and a template made from our own data. For all of the experiments, data are presented as mean ± SEM (*N* is number of animals). For statistics, physiological properties between Ts65Dn and 2N groups were compared using either Student's t-test for normalized data sets or ANOVA. Kolmogrov-Smirnov test was used for data sets that were not normally distributed unless otherwise noted. , and $P < 0.05$ was considered to be statistically significant.

Acknowledgments

This work was supported by The National Institute of Mental Health (MH65541 and MH56454), by the Down Syndrome Research and Treatment Foundation (DSRTF), as well as by the Larry L. Hillblom Foundation. This work was also supported by the Stanford University Center for Research and Treatment of Down Syndrome. We thank Craig Garner and William Mobley for their assistance and Scott Owen for reading the manuscript.

Abbreviations

DS	Down syndrome
GABA	y-amino butyric acid
IPSP/C	inhibitory postsynaptic potential/current
mIPSC	miniature inhibitory postsynaptic current
AMPA	2-amino-3-(5-methyl-3-oxo-1,2-oxazol-4-yl)propanoic acid
NMDA	N-methyl-D-aspartate
NBQX	2,3-dihydroxy-6-nitro-7-sulfamoyl-benzo[f]quinoxaline-2,3-dione
AP-5	(2R)-amino-5-phosphonovalerate
2N	diploid genotype
PPR	paired-pulse ratio

REFERENCES

Antonarakis SE, Lyle R, Dermitzakis ET, Reymond A, Deutsch S. Chromosome 21 and down syndrome: from genomics to pathophysiology. Nat Rev Genet. 2004; 5:725–738. [PubMed: 15510164]

Becker L, Mito T, Takashima S, Onodera K. Growth and development of the brain in Down syndrome. Prog Clin Biol Res. 1991; 373:133–152. [PubMed: 1838182]

Becker LE, Armstrong DL, Chan F. Dendritic atrophy in children with Down's syndrome. Ann Neurol. 1986; 20:520–526. [PubMed: 2947535]

Ben-Ari Y. Excitatory actions of gaba during development: the nature of the nurture. Nat Rev Neurosci. 2002; 3:728–739. [PubMed: 12209121]

Canfield MA, Honein MA, Yuskiv N, Xing J, Mai CT, Collins JS, Devine O, Petrini J, Ramadhani TA, Hobbs CA, Kirby RS. National estimates and race/ethnic-specific variation of selected birth

defects in the United States, 1999–2001. Birth Defects Res A Clin Mol Teratol. 2006; 76:747–756. [PubMed: 17051527]

Chakrabarti L, Best TK, Cramer NP, Carney RS, Isaac JT, Galdzicki Z, Haydar TF. Olig1 and Olig2 triplication causes developmental brain defects in Down syndrome. Nat Neurosci. 2010; 13:927–934. [PubMed: 20639873]

Contestabile A, Fila T, Ceccarelli C, Bonasoni P, Bonapace L, Santini D, Bartesaghi R, Ciani E. Cell cycle alteration and decreased cell proliferation in the hippocampal dentate gyrus and in the neocortical germinal matrix of fetuses with Down syndrome and in Ts65Dn mice. Hippocampus. 2007; 17:665–678. [PubMed: 17546680]

Davisson MT, Schmidt C, Reeves RH, Irving NG, Akeson EC, Harris BS, Bronson RT. Segmental trisomy as a mouse model for Down syndrome. Prog Clin Biol Res. 1993; 384:117–133. [PubMed: 8115398]

De Felipe J, Marco P, Fairen A, Jones EG. Inhibitory synaptogenesis in mouse somatosensory cortex. Cereb Cortex. 1997; 7:619–634. [PubMed: 9373018]

Fernandez F, Garner CC. Episodic-like memory in Ts65Dn, a mouse model of Down syndrome. Behav Brain Res. 2008; 188:233–237. [PubMed: 17950473]

Fernandez F, Morishita W, Zuniga E, Nguyen J, Blank M, Malenka RC, Garner CC. Pharmacotherapy for cognitive impairment in a mouse model of Down syndrome. Nat Neurosci. 2007; 10:411–413. [PubMed: 17322876]

Granholm AC, Sanders L, Seo H, Lin L, Ford K, Isacson O. Estrogen alters amyloid precursor protein as well as dendritic and cholinergic markers in a mouse model of Down syndrome. Hippocampus. 2003; 13:905–914. [PubMed: 14750653]

Guidi S, Bonasoni P, Ceccarelli C, Santini D, Gualtieri F, Ciani E, Bartesaghi R. Neurogenesis impairment and increased cell death reduce total neuron number in the hippocampal region of fetuses with Down syndrome. Brain Pathol. 2008; 18:180–197. [PubMed: 18093248]

Guihard-Costa AM, Khung S, Delbecque K, Menez F, Delezoide AL. Biometry of face and brain in fetuses with trisomy 21. Pediatr Res. 2006; 59:33–38. [PubMed: 16326987]

Hanson JE, Blank M, Valenzuela RA, Garner CC, Madison DV. The functional nature of synaptic circuitry is altered in area CA3 of the hippocampus in a mouse model of Down's syndrome. J Physiol. 2007; 579:53–67. [PubMed: 17158177]

Insausti AM, Megias M, Crespo D, Cruz-Orive LM, Dierssen M, Vallina IF, Insausti R, Florez J. Hippocampal volume and neuronal number in Ts65Dn mice: a murine model of Down syndrome. Neurosci Lett. 1998; 253:175–178. [PubMed: 9792239]

Jernigan TL, Bellugi U. Anomalous brain morphology on magnetic resonance images in Williams syndrome and Down syndrome. Arch Neurol. 1990; 47:529–533. [PubMed: 2139774]

Kates WR, Folley BS, Lanham DC, Capone GT, Kaufmann WE. Cerebral growth in Fragile X syndrome: review and comparison with Down syndrome. Microsc Res Tech. 2002; 57:159–167. [PubMed: 12112452]

Kleschevnikov AM, Belichenko PV, Villar AJ, Epstein CJ, Malenka RC, Mobley WC. Hippocampal long-term potentiation suppressed by increased inhibition in the Ts65Dn mouse, a genetic model of Down syndrome. J Neurosci. 2004; 24:8153–8160. [PubMed: 15371516]

Kullmann DM. Interneuron networks in the hippocampus. Curr Opin Neurobiol. 2011

Kurt MA, Kafa MI, Dierssen M, Davies DC. Deficits of neuronal density in CA1 and synaptic density in the dentate gyrus, CA3 and CA1, in a mouse model of Down syndrome. Brain Res. 2004; 1022:101–109. [PubMed: 15353219]

Larsen KB, Laursen H, Graem N, Samuelsen GB, Bogdanovic N, Pakkenberg B. Reduced cell number in the neocortical part of the human fetal brain in Down syndrome. Ann Anat. 2008; 190:421–427. [PubMed: 18722098]

Liu DP, Schmidt C, Billings T, Davisson MT. Quantitative PCR genotyping assay for the Ts65Dn mouse model of Down syndrome. Biotechniques. 2003; 35:1170–1174. 1176, 1178. passim. [PubMed: 14682051]

Lorenzi HA, Reeves RH. Hippocampal hypocellularity in the Ts65Dn mouse originates early in development. Brain Res. 2006; 1104:153–159. [PubMed: 16828061]

Marin-Padilla M. Pyramidal cell abnormalities in the motor cortex of a child with Down's syndrome. A Golgi study. J Comp Neurol. 1976; 167:63–81. [PubMed: 131810]

Nurse S, Lacaille JC. Do GABAA and GABAB inhibitory postsynaptic responses originate from distinct interneurons in the hippocampus? Can J Physiol Pharmacol. 1997; 75:520–525. [PubMed: 9250387]

Parker SE, Mai CT, Canfield MA, Rickard R, Wang Y, Meyer RE, Anderson P, Mason CA, Collins JS, Kirby RS, Correa A. Updated National Birth Prevalence estimates for selected birth defects in the United States, 2004–2006. Birth Defects Res A Clin Mol Teratol. 2010; 88:1008–1016. [PubMed: 20878909]

Parra P, Gulyas AI, Miles R. How many subtypes of inhibitory cells in the hippocampus? Neuron. 1998; 20:983–993. [PubMed: 9620702]

Pennington BF, Moon J, Edgin J, Stedron J, Nadel L. The neuropsychology of Down syndrome: evidence for hippocampal dysfunction. Child Dev. 2003; 74:75–93. [PubMed: 12625437]

Pinter JD, Brown WE, Eliez S, Schmitt JE, Capone GT, Reiss AL. Amygdala and hippocampal volumes in children with Down syndrome: a high-resolution MRI study. Neurology. 2001a; 56:972–974. [PubMed: 11294940]

Pinter JD, Eliez S, Schmitt JE, Capone GT, Reiss AL. Neuroanatomy of Down's syndrome: a high-resolution MRI study. Am J Psychiatry. 2001b; 158:1659–1665. [PubMed: 11578999]

Pollonini G, Gao V, Rabe A, Palminiello S, Albertini G, Alberini CM. Abnormal expression of synaptic proteins and neurotrophin-3 in the Down syndrome mouse model Ts65Dn. Neuroscience. 2008; 156:99–106. [PubMed: 18703118]

Reeves RH. Down syndrome mouse models are looking up. Trends Mol Med. 2006; 12:237–240. [PubMed: 16677859]

Siarey RJ, Carlson EJ, Epstein CJ, Balbo A, Rapoport SI, Galdzicki Z. Increased synaptic depression in the Ts65Dn mouse, a model for mental retardation in Down syndrome. Neuropharmacology. 1999; 38:1917–1920. [PubMed: 10608287]

Siarey RJ, Stoll J, Rapoport SI, Galdzicki Z. Altered long-term potentiation in the young and old Ts65Dn mouse, a model for Down Syndrome. Neuropharmacology. 1997; 36:1549–1554. [PubMed: 9517425]

Takashima S, Becker LE, Armstrong DL, Chan F. Abnormal neuronal development in the visual cortex of the human fetus and infant with down's syndrome. A quantitative and qualitative Golgi study. Brain Res. 1981; 225:1–21. [PubMed: 6457667]

Takashima S, Ieshima A, Nakamura H, Becker LE. Dendrites, dementia and the Down syndrome. Brain Dev. 1989; 11:131–133. [PubMed: 2523670]

Tyzio R, Represa A, Jorquera I, Ben-Ari Y, Gozlan H, Aniksztejn L. The establishment of GABAergic and glutamatergic synapses on CA1 pyramidal neurons is sequential and correlates with the development of the apical dendrite. J Neurosci. 1999; 19:10372–10382. [PubMed: 10575034]

Whittle N, Sartori SB, Dierssen M, Lubec G, Singewald N. Fetal Down syndrome brains exhibit aberrant levels of neurotransmitters critical for normal brain development. Pediatrics. 2007; 120:e1465–e1471. [PubMed: 17998315]

Winter TC, Ostrovsky AA, Komarniski CA, Uhrich SB. Cerebellar and frontal lobe hypoplasia in fetuses with trisomy 21: usefulness as combined US markers. Radiology. 2000; 214:533–538. [PubMed: 10671607]

Wisniewski KE. Down syndrome children often have brain with maturation delay, retardation of growth, and cortical dysgenesis. Am J Med Genet Suppl. 1990; 7:274–281. [PubMed: 2149962]

Zucker RS, Regehr WG. Short-term synaptic plasticity. Annu Rev Physiol. 2002; 64:355–405. [PubMed: 11826273]

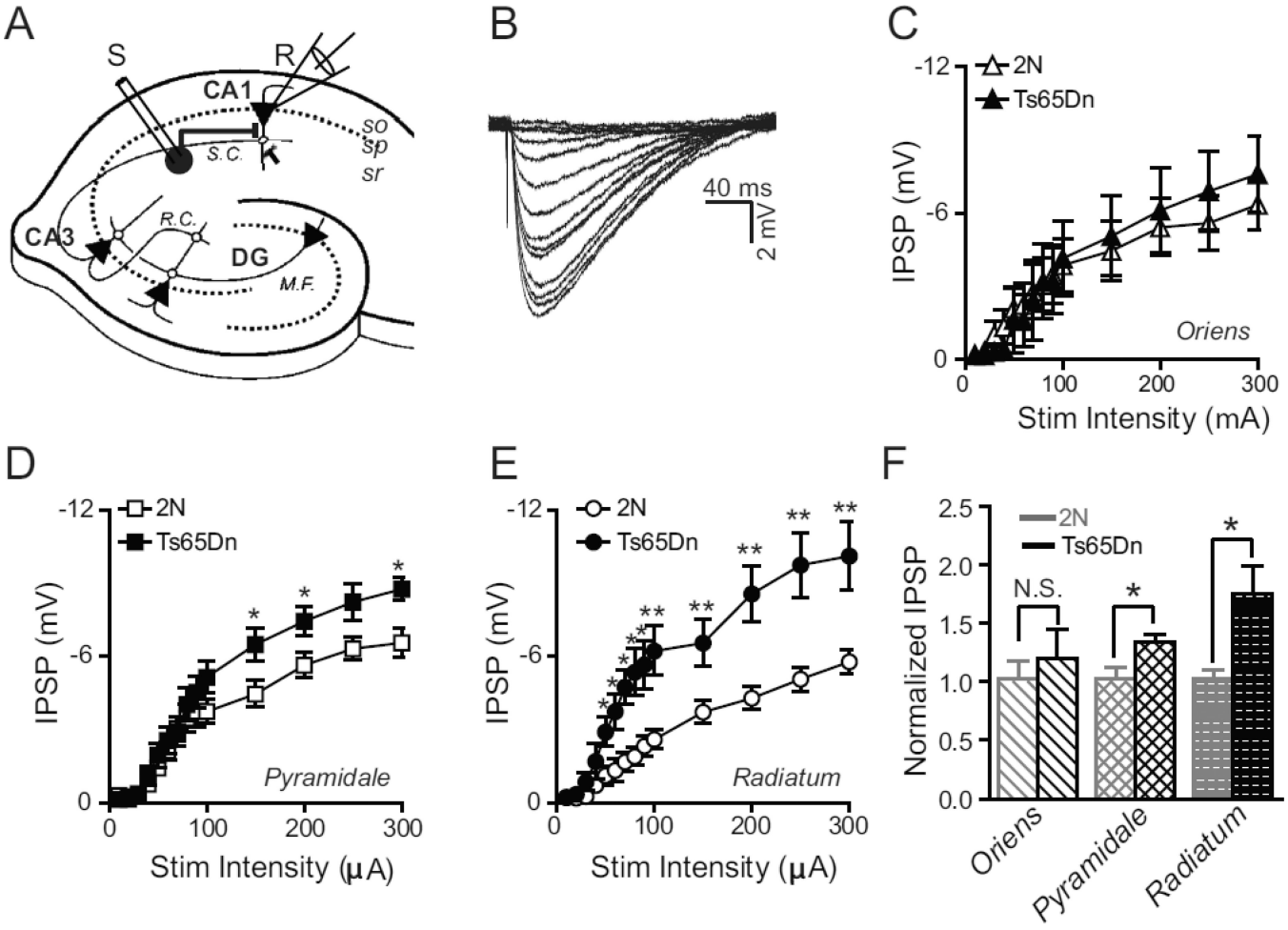

Figure 1. Layer Specific Alteration in Evoked Monosynaptic Inhibition

(A) Schematic of the hippocampal slice with the whole-cell recording configuration in the CA1 region. Inhibitory interneuron circle in *stratum radiatum* (sr) of CA1 is stimulated by extracellular stimulating electrode (S) while the inhibitory response is measured from a CA1 pyramidal neuron (triangle) in the *stratum pyramidale* (*sp*) by the recording electrode (R). M.F.-mossy fibers, DG-dentate gyrus, R.C.-recurrent collaterals, S.C.-Schaffer collaterals.

(B) Example traces of evoked postsynaptic inhibitory potentials (IPSP) recorded from a CA1 pyramidal neuron in response to various stimulation intensities ranging from 10–300 μA delivered in the *stratum radiatum*.

(C–E) Plots of evoked IPSP amplitude as a function of stimulus amplitude when the stimulation electrode is placed in the *stratum oriens* (C), *pyramidale* (D), and *radiatum* (E), respectively. There was a significant excess of evoked inhibition in Ts65Dn animals as compared to 2N littermates when the stimulating electrode was placed in *s. radiatum* (E) and *s. pyramidale* (D) but not in *s. oriens* (C). 2N, n=8; Ts65Dn, n=7, where 'n' refers to the total number of animals; *P <0.05; **P <0.001, ANOVA). Error bars represent SEM.

(F) Inhibitory synaptic strength in Ts65Dn and 2N animals, in each layer, normalized to the average maximal synaptic strength (at 300 μA stimulation intensity) in 2N animals. * P <0.03; unpaired, two-tailed *t*-test. Error bars represent SEM.

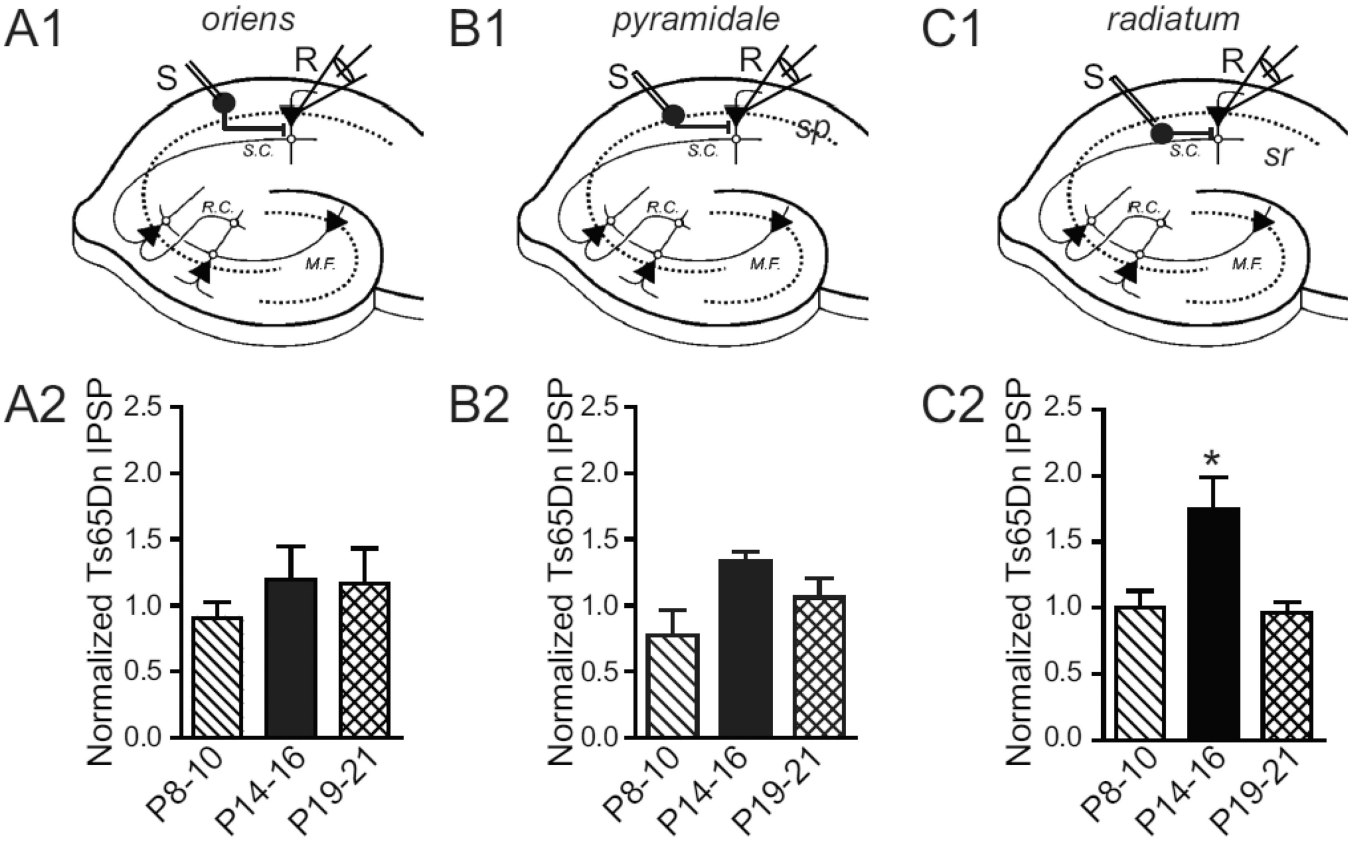

Figure 2. Developmental Time course of Synaptic Inhibition

(A1–C1) Schematic diagrams depicting the placement of stimulating and recording electrode in the CA1 region. Inhibitory interneurons in *s. oriens* (*so*, A1), *s. pyramidale* (*sp*, B1), and *s. radiatum* (*sr*, C1), respectively, are stimulated by an extracellular stimulating electrode (S) while the inhibitory response is measured from a CA1 pyramidal neuron by the recording electrode (R). (A2–C2) The mean IPSP amplitude in response to 300 μA Stimulation Intensity in Ts65Dn animals normalized to the age-matched mean IPSP in 2N littermates, shown at different developmental times: P8–10, P14–16, and P19–21 for *s. oriens* (A2), *s. pyramidale* (B2), and *s. radiatum* (C2), respectively. The mean inhibitory synaptic strength of Ts65Dn animals normalized to 2N littermates is significantly greater at ages P14–16 and is observed only when stimulating inhibitory interneurons and/or their axons located in the *s. radiatum* ($P < 0.05$, *t - test*). P8–10; n=6, 2N; n=5, Ts65Dn; P14–16; n=8, 2N; n=7, Ts65Dn; P19-P21; n=7, 2N; n=7, Ts65Dn, where ‘n’ refers to the total number of animals in each age group.

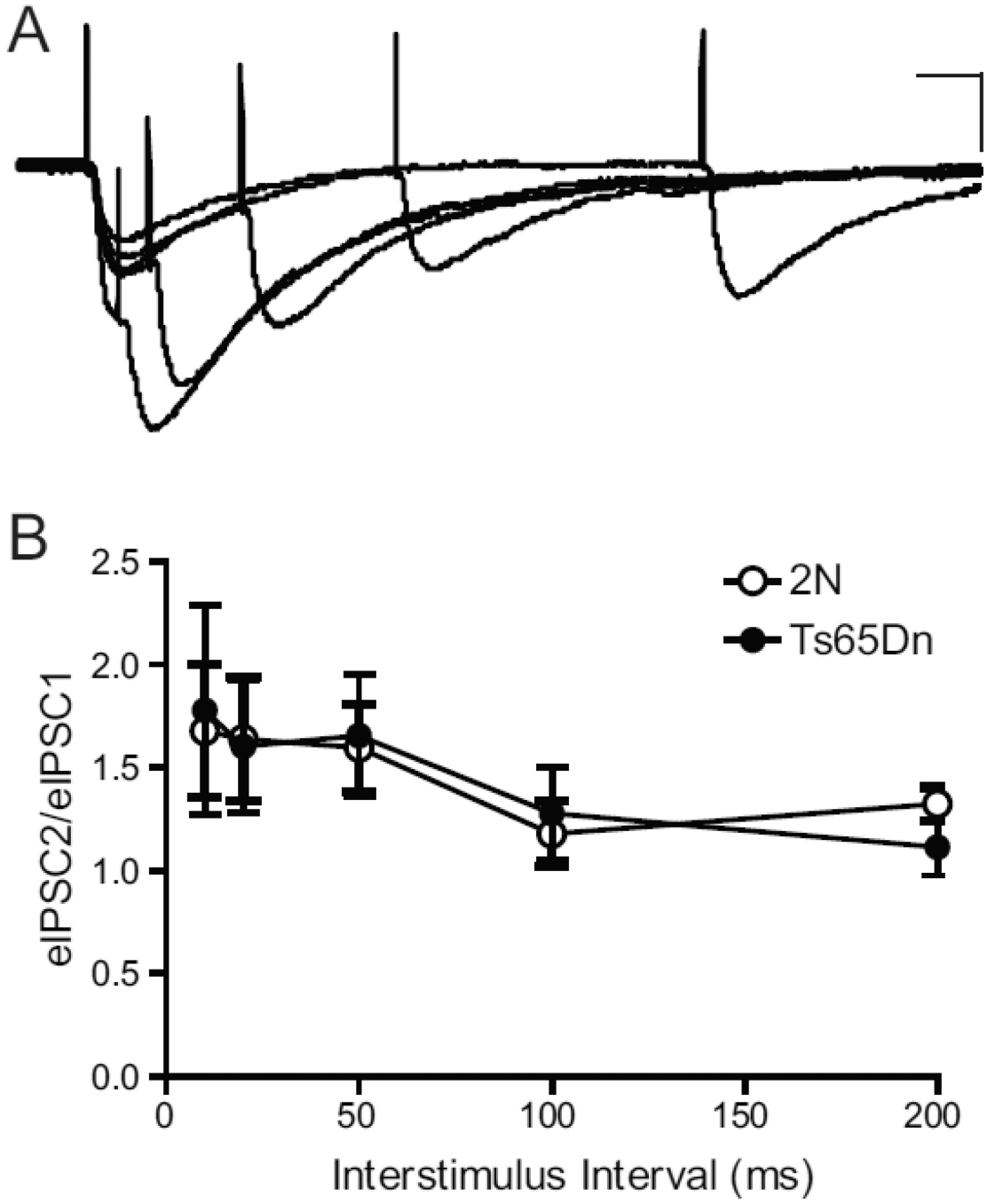

Figure 3. No Change in Relative Release Probability

Paired-pulse facilitation of evoked IPSCs was similar in slices from Ts65Dn and 2N mice under conditions of low extracellular calcium (0.8mM).

(A) Representative IPSCs evoked in CA1 pyramidal neurons in slices from Ts65Dn mice. Inter-stimulus intervals varied from 10 to 200 ms. Scale bars for traces are 50 pA, 20 ms.

(B) The averaged ratios of amplitudes for the first and second responses (i.e., eIPSC2/eIPSC1) in 2N and Ts65Dn slices. Open bar, 2N (n=5); filled bar, Ts65Dn (n=4), where ‘n’ refers to the total number of animals. The error bars in B represent SEM.

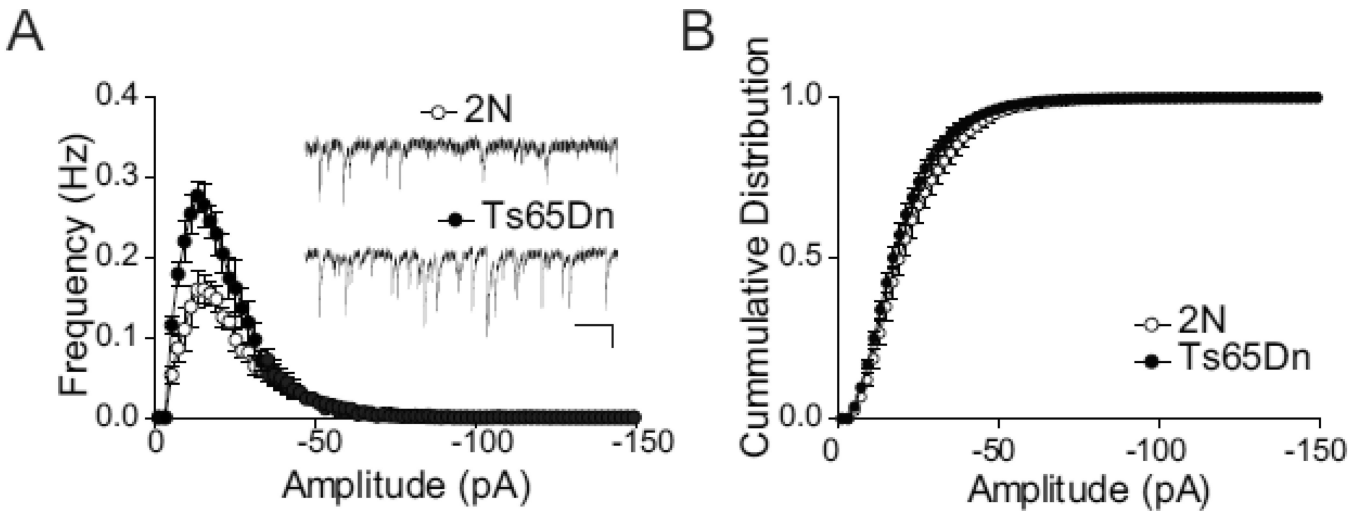

Figure 4. Increased Frequency of Spontaneous Miniature IPSCs in Ts65Dn

(A) Frequency histograms of miniature IPSCs recorded in the presence of TTX (1μM), NBQX (10 μM) and AP5 (50 μM). Each histogram represents average mIPSCs (1 pA bins, means ± SEM) from n=7, 2N and n=5, Ts65Dn, where 'n' represents the number of animals used and is an average of recordings from 1–3 slices per animal. The total frequency of mEPSCs was significantly increased in recordings from Ts65Dn compared with 2N mice (unpaired Student's *t* test, $P < 0.05$). Open circles are events collected from 2N slices, closed circles from Ts65Dn slices. Scale bars for inset traces are 20 pA, 500 ms.

(B) Cumulative histogram of mIPSC amplitude. No difference in mIPSC amplitude was noted between the 2N and Ts65Dn groups. Open circles, 2N; filled circles, Ts65Dn. The error bars in A and B represent SEM.